If a man will begin with certainties, he shall end in doubts; but if he will be content to begin with doubts he shall end in certainties.

Francis Bacon (1605)

3

Methodology

3 METHODOLOGY

In this chapter a methodology is formulated to test the main research hypothesis that the accuracy of design models for UTCRCP can benefit from the adoption of fracture mechanics concepts. The methodology is developed taking cognizance of the state of existing knowledge presented in Chapter 2.

The methodology chapter comprises three main sections. The first section on the research design delineates the approaches used to test the hypothetical propositions of this work. In Section 3.2, the structure of the experimental work is discussed as well. The selection of test methods and the experimental setup used for the study is described. To obtain a reliable estimate of the tensile strength of the fibre reinforced material, an adjusted tensile splitting procedure was developed. The FEM based numerical methodologies used in the study are discussed in Section 3.3.

3.1 Research design

The test of the main hypothesis, formulated in Chapter 1, lies in the validation of the set of three hypothetical sub-propositions.

The first of the propositions is that the high performance fibre reinforced concrete material will exhibit a strong size effect due to its distinctly non-linear behaviour in fracture. This is tested by means of laboratory experiments on specimens of different sizes. The results will be

compared to published size effect data for plain concrete. Bažant and Planas (1997) have summarized the results of size effect studies on plain concrete. A range of different test methods have been used by various researchers. The most common test configurations are the Three Point Bending (TPB) and Four Point Bending (FPB) flexural beam setup. The TPB and FPB tests are the main approaches used to explore size effect of the UTCRCP as part of this study. Testing on different sized circular panels is done as well to compare the size effect results for different geometries.

If the first proposition is supported by the experimental data, this will imply that the reliability of MOR, obtained for a specific specimen size and geometry, as a predictor of the peak load of elements of a different size and or geometry, is limited.

The second proposition states that, in contrast to the MOR, fracture mechanics can be used to more accurately and precisely predict the peak load and flexural behaviour of elements of a different size and geometry. This hypothesis is tested by numerically simulating the flexural experiments using fracture mechanics. The fracture mechanics parameters are determined for a certain specimen size and geometry and based on this a fracture mechanics model is defined for the material. The validation of the hypothesis depends on the predictive performance of the fracture mechanics model for the fracture behaviour of different sizes and geometry, in comparison to the performance of a MOR based design approach.

The final proposition pertains to the prediction of the fatigue performance of the material. It states that the accuracy, and possibly the precision, of fatigue prediction models can be improved through the use of fracture mechanics concepts. To test this hypothesis, prediction models are calibrated based on cyclic flexural tests on beams. These models are then applied to predict the fatigue performance of beams of different sizes and of centrally loaded circular panels. The precision of the models developed using the conventional approach is compared to the performance of models developed based on fracture mechanics concepts.

A requirement for the envisaged methodology is that the parameters can be determined using robust test methods that can be applied by the industry on a routine basis.

3.2 Experimental program and methods

The experimental work for this study took place in four consecutive phases. Three of the test phases were conducted at the University of Pretoria (UP). These phases focussed on the material behaviour of fibre reinforced concrete. One phase of testing took place at the University of California at Davis (UC Davis). In this phase an initial exploration of the relationship between the behaviour of plain concrete under monotonic and dynamic fatigue loading was conducted. The timeline, test configuration and objectives of the different phases are shown in Figure 3-1.

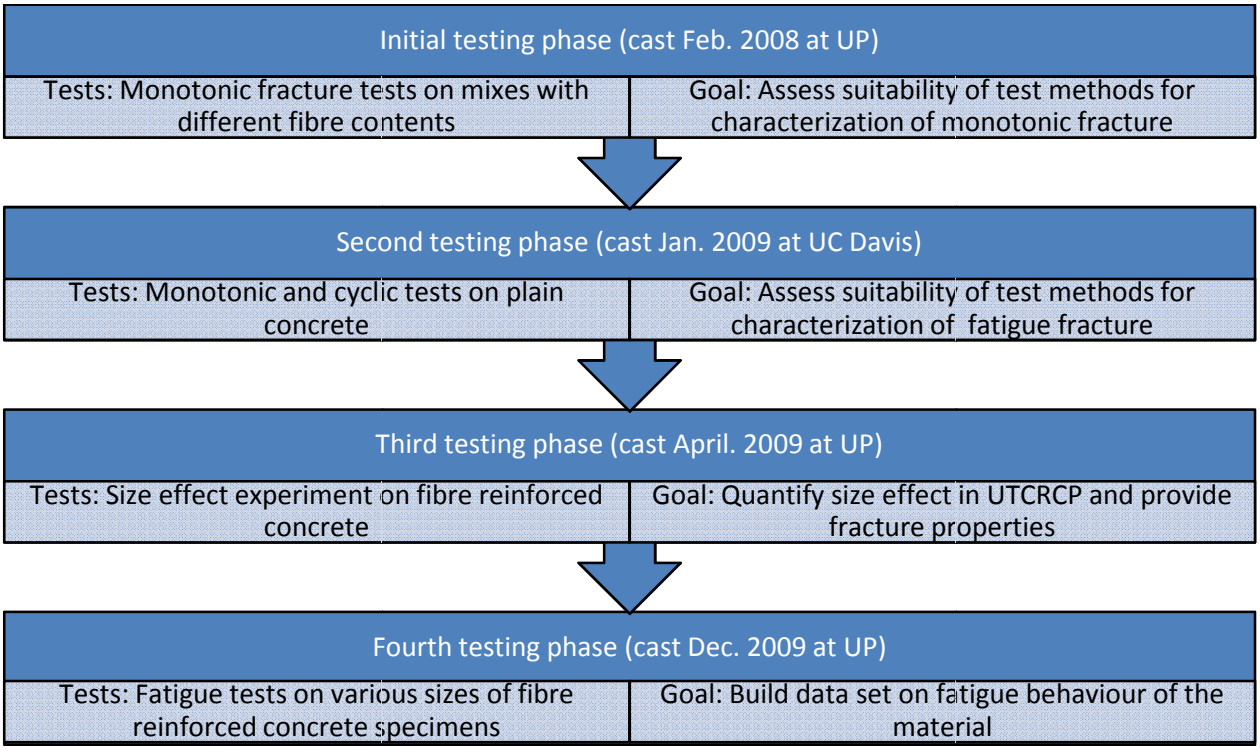

Figure 3-1: Timeline and objectives of experimental phases

The first two phases were aimed at identifying suitable test methods for the characterization of the fracture behaviour of the material under monotonic and cyclic loading. The focus in these phases was on the determination of fracture properties from the monotonic tests which could be used in fracture mechanics models.

After the test and analysis methods were developed, a size effect study on the high performance fibre reinforced material was performed in phase three.

Finally, in phase four, cyclic testing was performed in conjunction with monotonic experiments. The aim was to build a data set against which the fatigue models could be calibrated.

Each phase contains a different set of flexural tests to suit the specific objectives of that phase. The flexural test setup and mix designs are discussed per phase in the following sections. In every phase further experiments were performed as part of quality control, to determine general engineering properties and the tensile strength of the materials. These tests, reoccurring in every phase, are discussed in separate sections.

3.2.1 Phase I determining fracture properties of fibre reinforced concrete

The first mixes were cast in February 2008 at the University of Pretoria. The aim of the initial testing phase was to obtain and compare the fracture properties of two mixes. In terms of the propositions of this study, the results from this round of testing were used to develop fracture mechanics models and to show that these models can be used to predict the flexural behaviour of the material.

One mix was prepared with 80 kg/m^3 steel fibres, the other with a steel fibre content of 120 kg/m^3. The components by mass for the mix designs are shown in Table 3-1. The designs are typical for the designs used in the construction of UTCRCP.

The first round of testing was in many ways an explorative study to determine the optimum test methods for the determination of fracture properties. Beams of various sizes and geometry were tested in TPB and FPB test configurations. To investigate fracture in a three dimensional test, a centrally loaded panel circular panel on three support points was used. Table 3.2 and Table 3.3 show the dimensions of the specimens cast as part the first phase for Mixes A and B respectively. The table lists the mix type, the dimensions of the specimen and the identifier per specimen type. Individual specimens would be numbered TPB1-A-1,2,3, etc.

Table 3-1: Mix components by mass first round of testing

Component	**Type**	**Mix A [kg/m^3]**	**Mix B [kg/m^3]**
Cement	Cem I 42.5 R	450.3	448.0
Coarse aggregate	Quartzite [4.75 mm - 6.7 mm]	930.6	925.9
Fine aggregate	Quartzite [0.00 mm - 4.75 mm]	725.5	721.8
Water		170.7	169.8
Steel Fibres	Bekaert Dramix [30 mm x 0.5 mm]	80.1	119.5
Polypropylene Fibre	[12 mm]	2.0	2.0
Admixture	P100	4.0	4.0
Admixture	O100	2.5	2.5
Silica Fume (CSF)	Witbank	65.0	64.7
Fly ash	Lethabo	80.1	79.6

Table 3-2: Specimen dimensions mix A

Identifier (ID)	Type	Length (L) / Diameter (D) [mm]	Height (h) [mm]	Width (b) [mm]	Span (s) [mm]	Notch (a) [mm]	Rebar	Number cast
TPB1-A	TPB	550	150	150	500	25	-	3
TPB2-A	TPB	550	125	150	500	-	-	3
TPB3-A	TPB	550	75	150	500	25	-	3
TPB4-A	TPB	550	50	150	500	-	-	3
TPB5-A	TPB	550	150	150	500	25	3Y5.6	3
TPB6-A	TPB	550	125	150	500	-	3Y5.6	3
TPB7-A	TPB	550	75	150	500	25	3Y5.6	3
TPB8-A	TPB	550	50	150	500	-	3Y5.6	3
FPB1-A	FPB	750	150	150	600	-	-	3
FPB2-A	FPB	750	150	150	600	-	3Y5.6	3
Cu-A	Cube	100	100	100	-	-	-	12
Cyl1-A	Cylinder	150	300	-	-	-	-	3
Cyl2-A	Cylinder	75	300	-	-	-	-	3
Disk1-A	Disk	600	55	-	-	-	-	3
Disk2-A	Disk	800	70	-	-	-	-	3
Disk3-A	Disk	600	55	-	-	-	50x50x5.6 [1]	3
Disk4-A	Disk	800	70	-	-	-	50x50x5.6 [1]	3

Notes: [1] mesh reinforcement

Table 3-3: Specimen dimensions mix B

Identifier (ID)	Type	Length (L) / Diameter (D) [mm]	Height (h) [mm]	Width (b) [mm]	Span (s) [mm]	Notch (a) [mm]	Rebar	Number cast
TPB1-B	TPB	550	125	150	500	-	-	3
TPB2-B	TPB	550	75	150	500	25	-	3
TPB3-B	TPB	550	50	150	500	-	-	3
TPB4-B	TPB	550	125	150	500	-	3Y5.6	3
TPB5-B	TPB	550	75	150	500	25	3Y5.6	3
TPB6-B	TPB	550	50	150	500	-	3Y5.6	3
FPB1-B	FPB	750	150	150	600	-	-	3
FPB1-B	FPB	750	150	150	600	-	3Y5.6	3
Cu-B	Cube	100	100	100	-	-	-	12
Cyl1-B	Cylinder	150	300	-	-	-	-	3
Cyl2-B	Cylinder	75	300	-	-	-	-	3
Disk1-B	Disk	600	55	-	-	-	-	3
Disk2-B	Disk	800	70	-	-	-	-	3

The procedure for TPB to determine fracture properties as recommended by RILEM technical committee 162-TDF (RILEM, 2002) was used as the point of departure for the TPB tests. Besides the standard recommended beams of 150 mm x 150 mm cross section with a 550 mm length and a 25 mm notch, a number of other specimen sizes and geometries were used. The reason for using different cross-sections is that the typical application thickness of the UTCRCP is 50 mm. Samples with and without a notch were also included to investigate the suitability of the eventual numerical models for fracture simulation for cases with and without a pre-formed crack. A schematic representation of the TPB test setup can be found in Figure 3-2a. A picture of the TPB test setup used at the University of Pretoria is shown in Figure 3-3a.

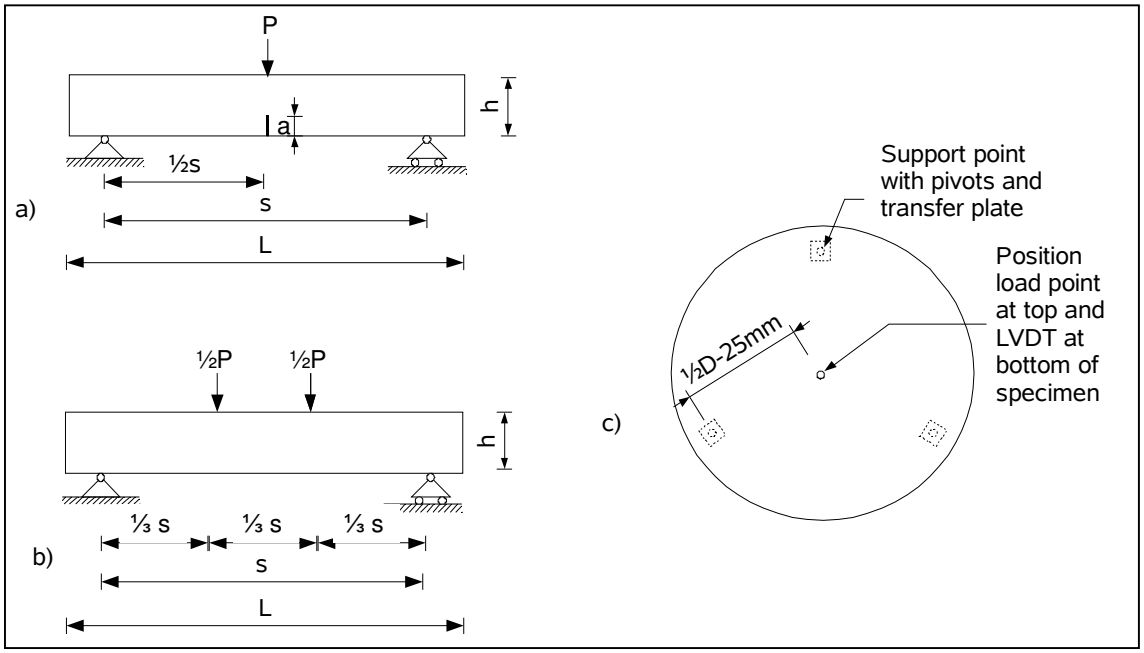

Figure 3-2a) TPB test setup, b) FPB test setup, c) Disk test configuration

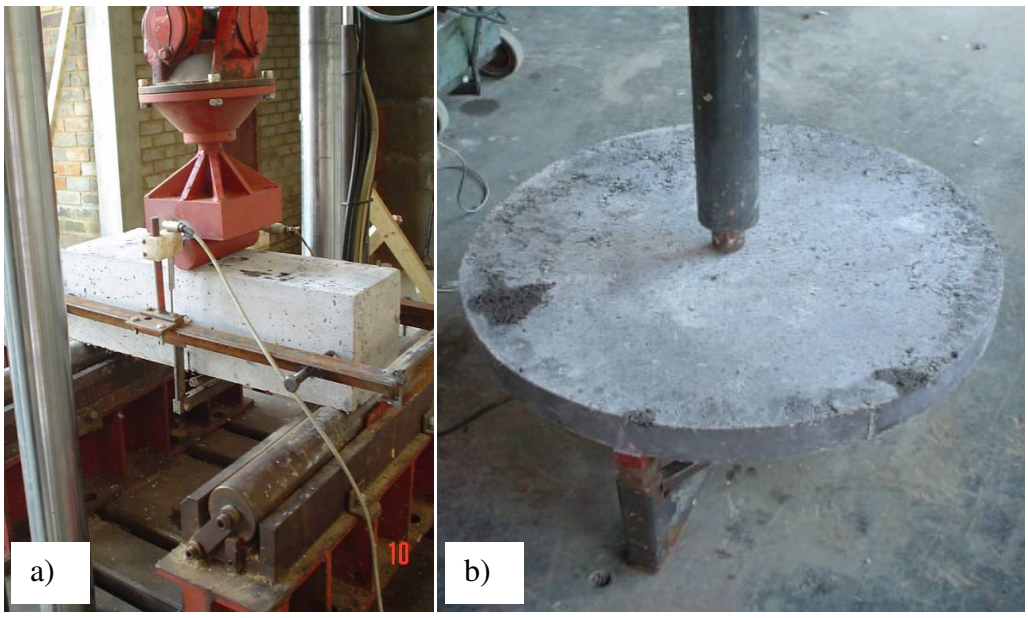

Figure 3-3a) Picture of TPB setup, b) picture of disk test setup

The FPB tests were performed on specimens without notch in accordance with Japanese test method JCI SF 4 (JCI, 1983). This test method had been used previously by Elsaigh (2007) at the University of Pretoria to successfully describe the post cracking behaviour of fibre reinforced concrete. The FPB test configuration is shown in Figure 3-2b.

In both the TPB and FPB tests the vertical displacement at mid-span was recorded by means of Linear Variable Displacement Transducers (LVDT) at either side of the beam. The reference frame for the displacement was mounted at half height of the beam specimen and mid-span displacement was measured relative to reference points above the supports. The reference frame can be seen in Figure 3-3a.

The test method for the centrally loaded concrete disks was performed in accordance with ASTM standard test method C 1550 – 05 (ASTM, 2005). Apart from the standard 800 mm diameter, 70 mm thick specimen dimension as prescribed by the standard, smaller 600 mm diameter, 55 mm thick specimens were also tested. In this test the flexural response of a centrally loaded concrete disk supported on three pivot points is measured. Figure 3-2c shows the test setup. A picture of the test is shown in Figure 3-3b. The vertical displacement is measured with an LVDT placed under the disk in line with the position of the loading point at the top of the disk. The test method is used routinely at the University of Pretoria to characterize the flexural strength of UTCRCP material (Kearsley and Mostert, 2010).

Half of the beam samples prepared at each steel fibre content contained three 5.6 mm diameter reinforcement bars. Half of the disk specimens contained a 50 mm x 50 mm x 5.6 mm mesh. The tensile yield strength (f_t) of the bars was determined in direct tensile tests as 550 MPa. The rebar was included to capture the effect of the mesh reinforcement built-in at half depth in the UTCRCP layer. The reinforcement bars were placed with 25 mm cover to either, the bottom of the specimen or, for notched specimen, the top of the notch.

All tests were run in displacement control, at the loading rates prescribed by the respective standard test methods.

An important finding from this round of testing for the subsequent experimental phases, was that fracture properties are best determined from notched TPB specimens in tests run up to high displacements.

3.2.2 Phase II fracture properties of concrete under monotonic and cyclic loading

The second phase of testing took place at the University of California, Davis (UC Davis), during an eight month work visit of the author to this university. The aim of the tests at UC Davis was to compare the fracture behaviour of concrete cyclic loading with the behaviour

under monotonic loading. During this phase the methodology to study the fatigue behaviour of concrete in flexural experiments was developed. The monotonic test results were used to further developed the fracture mechanics models and the TPB test procedure.

A plain concrete mix was used for this purpose. The mix design shown in Table 3-4 is a typical design for Portland Cement Concrete (PCC) pavements in the state of California. The specimens were cast in January 2009.

The specimen dimensions are shown in Table 3.5. To ensure stability of the TPB tests up to high displacements, a self-weight corrected geometry was used. The length of the specimens is twice the size of the span, thus ensuring that no collapse under self-weight occurs near the end of the test. The test setup at UC Davis is shown Figure 3-4a and b.

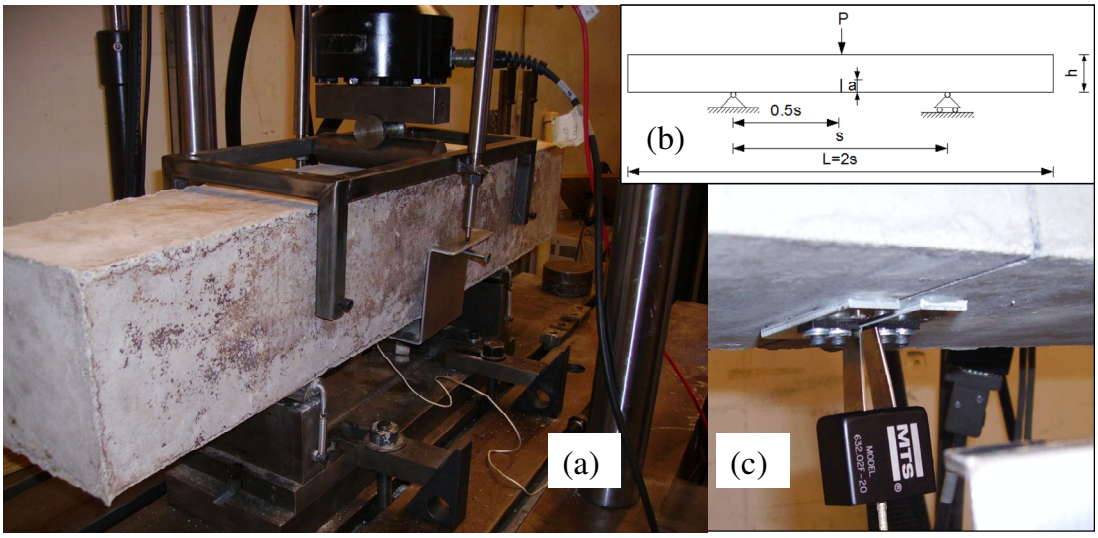

Figure 3-4a and b) TPB test configuration at UC Davis, c) Detail of the knife edges and clip gauge.

The vertical displacement was measured using LVDTs on either side of the beam in a similar fashion as was done earlier during the tests at UP. In addition to the vertical displacement, the opening of the crack was measured by means of a clip gauge mounted to knife edges on either side of the notch. A detail of the clip gauge measuring the Crack Mouth Opening Displacement (CMOD) is shown in Figure 3-4c. The clip gauge allows a more sensitive measurement of the fracture behaviour of the specimens. The range of the clip gauge is

however, limited to about 5 mm, therefore the vertical LVDTs are relied upon to measure the behaviour at larger displacements.

The loading rate for the monotonic tests was set to 0.5 mm per minute, which is equal to the loading rate used during the experiments at UP. The fatigue tests were performed in load control. A haversine loading was applied at a frequency of 4 Hz. The loading amplitude was set to various percentages of the peak load obtained in the monotonic tests. The load-displacement response in terms of vertical displacement and CMOD was recorded at sampling rates of at least 10 Hz.

Table 3-4: Mix components by mass testing at UC Davis

Component	Type	[kg/m^3]
Cement	Type II-V	306.9
Coarse aggregate	Granite [19 mm- 38 mm]	593.7
Coarse aggregate	Granite [4.75 mm – 25 mm]	593.7
Fine aggregate	Granite [0.00 mm -4.75 mm]	768.8
Water		168.0

Table 3-5: Specimen dimensions mix C

Identifier (ID)	Type	Length (L) / Diameter (D) [mm]	Height (h) [mm]	Width (b) [mm]	Span (s) [mm]	Notch (a) [mm]	Number cast
TPB1-C	TPB	914.4	152.4	152.4	457.2	50.8	3
TPBF1-C	TPB fatigue	914.4	152.4	152.4	457.2	50.8	9
Cyl1-C	Cylinder	150	300	-	-	-	14

The results showed that the use of weight corrected specimens in the TPB test allows for stable tests up to high deflections. This approach was used in the subsequent test phases to obtain a better measure of the fracture properties of the materials.

3.2.3 Phase III Size-effect in fibre reinforced concrete

In April 2009 specimens were cast at UP cast for a third round of testing. The objective was to investigate size-effect in fibre reinforced concrete. Weight corrected TPB specimens were cast, using the mix design shown in Table 3-6. The mix contained 120 kg/m^3 steel fibres. Beam specimens of three different sizes were cast while maintaining the geometry. In other words, the depth to span and notch to depth ratios were kept constant for all sizes. The beam

geometry is as shown in Figure 3-4c. In this round of testing the combination of a frame with LVDTs to monitor vertical displacement and a clip gauge to measure the CMOD was again used. Once the specimens were broken in the TPB tests, the halves were tested again in FPB test configuration (as shown in Figure 3-2b), thus providing an indication of size effect in both TPB and FPB. The smallest, 50 mm deep, specimens could not be tested in FPB due to the fact that their span was too short for the testing equipment. Since the FPB test specimens do not contain a notch vertical displacement only was measured during the tests. All tests were run in displacement control at a constant displacement rate of 0.5 mm per minute.

Table 3-6: Mix components by mass mix D

Component	Type	[kg/m^3]
Cement	Cem I 42.5R	464.5
Coarse aggregate	Quartzite [4.75 mm - 6.7 mm]	865.9
Fine aggregate	Quartzite [0.00 mm - 4.75 mm]	750.5
Water		176.1
Steel Fibres	Bekaert Dramix [30 mm x 0.5 mm]	120.2
Polypropylene Fibre	[12 mm]	2.0
Admixture	O100	4.4
Admixture	P100	3.0
Silica Fume (CSF)	Witbank	63.8
Fly ash	Lethabo	78.5

Table 3-7: Specimen dimensions mix D

Identifier (ID)	Type	Length (L) / Diameter (D) [mm]	Height (h) [mm]	Width (b) [mm]	Span (s) [mm]	Notch (a) [mm]	Number cast
TPB1-D	TPB	330	50	150	165	16.5	3
TPB2-D	TPB	1000	150	150	500	50	3
TPB3-D	TPB	1500	225	150	750	75	3
FPB1-D	FPB	500	150	150	450	-	3
FPB2-D	FPB	750	225	150	675	-	3
Cu-D	Cube	100	100	100	-	-	9
Cyl1-D	Cylinder	150	300	-	-	-	9

3.2.4 Phase IV fatigue in fibre reinforced concrete.

The final set of specimens were cast in December 2009 at UP. The main aim of this experimental phase was to explore the fatigue behaviour of the high performance fibre reinforced concrete under cyclic loading. Specimens of various sizes were cast to investigate the occurrence of size effect in fatigue. For each size a set of specimens was cast for

monotonic testing as well. The monotonic testing was included to further explore size effect, to determine the static fracture properties and to compare the fracture results from monotonic experiments to the fatigue behaviour of the material. The test results from this phase provided the data set for the development of conventional and fracture mechanics based fatigue models. The mix design containing 80 kg/m^3 steel fibres is shown in Table 3-8.

Table 3-8: Mix components by mass mix E

Component	**Type**	**[kg/m^3]**
Cement	Cem II 52.5 N	450.0
Coarse aggregate	Dolomite [4.75 mm – 9.5 mm]	950.0
Fine aggregate	Dolomite [0.00 mm - 4.75 mm]	900.0
Water		165.0
Steel Fibres	Bekaert Dramix [30 mm x 0.5 mm]	80.0
Polypropylene Fibre	[12 mm]	2.0
Admixture	O100	4.0
Admixture	P100	4.0
Silica Fume (CSF)	Witbank	50.0

TPB, FPB and disk specimens were cast as part of this experimental phase. An overview of the specimen types is provided in Table 3-9. TPB samples were produced with the weight corrected geometry shown in Figure 3-4c. TPB specimens were tested under monotonic loading only to obtain fracture mechanics properties for the mix. Both the vertical displacement and the CMOD were measured during the tests using the same procedure as in the previous two phases. The FPB and centrally loaded disk specimens were tested under both monotonic and cyclic loading. The peak load was obtained from the monotonic tests and the cyclic loads and the cyclic test were run at different ratios of the average monotonic peak load.

Table 3-9: Specimen dimensions mix E

Identifier (ID)	Type	Length (L) / Diameter (D) [mm]	Height (h) [mm]	Width (b) [mm]	Span (s) [mm]	Notch (a) [mm]	Number cast
TPB1-E	TPB	900	150	150	450	50	10
FPB1-E	FPB	500	150	150	450	-	10
FPB2-E	FPB	350	100	100	300	-	5
FPB3-E	FPB	200	50	50	150	-	5
FPBF1-E	FPB fatigue	500	150	150	450	-	20
FPBF2-E	FPB fatigue	350	100	100	300	-	20
FPBF3-E	FPB fatigue	200	50	50	150	-	20
Disk1-E	Disk	600	55	-	-	-	3
DiskF1-E	Disk fatigue	600	55	-	-	-	18
Cu-E	Cube	100	100	100	-	-	12
Cyl1-E	Cylinder	150	300	-	-	-	12

The vertical displacement was measured at a sampling rate of 10 Hz during both monotonic and cyclic FPB tests. The monotonic tests in both TPB and FPB setup were run in displacement control at a constant displacement rate of 0.5 mm per minute. The cyclic tests were run in load control, the haversine loading was applied at a frequency of 2 Hz. Figure 3-5 shows the test setup for the smallest of the FPB specimen types.

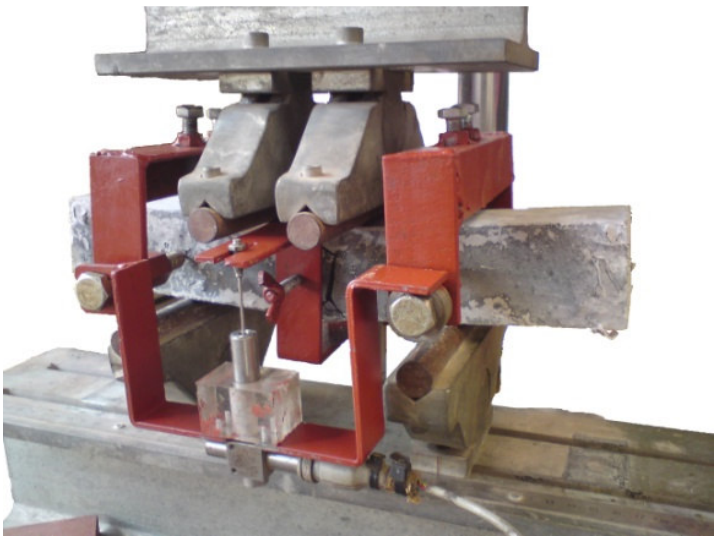

Figure 3-5: Picture of test setup for FPB3-E and FPB3F-E

The monotonic load experiments on the disk specimens were performed using the procedures as discussed for the first testing phase. The cyclic loading tests were conducted using a haversine load wave at a frequency of 2 Hz.

3.2.5 Determining engineering properties

In each test phase, specimens were cast to determine the compressive strength (f_c) as a quality control measure. Specimens were also produced to determine static modulus of elasticity E and Poisson's ratio υ. The static E and υ are used as material properties for the linear elastic part of the material behaviour in the numerical simulations performed as part of this study. The tests were performed in accordance with local test methods. At the University of Pretoria the compressive strength tests were performed on cubes (denoted "Cu" in the specimen tables of the previous section) in accordance with British Standard BS 1881 (BSI, 1983). Cylindrical specimens (denoted "Cyl1-C" in Table 3-5) were used to determine the compressive strength at UC Davis in accordance with ASTM C 39 (ASTM, 2008a) At both universities the tests to determine E and υ were performed in accordance with the standard procedures contained in ASTM C469-02 (ASTM, 2008b).

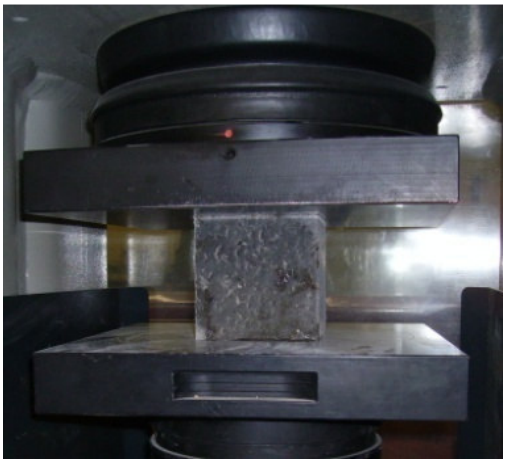

Figure 3-6: Compressive strength test setup at UP

3.2.6 Determining tensile strength

The tensile strength (f_t) is a key material parameter for fracture mechanics based analysis of concrete structures. It is generally determined using either a direct tensile test or splitting

tensile test setup. Both tests are simple in concept, but have proven quite complicated to run in such a way that reliable results, independent of specimen size and boundary conditions, are obtained. Additional challenges occur when the aim is to obtain a reliable measure of f_t for FRC, as is the case in this study.

The complexity of the direct tensile test concerns mainly the selection of specimen size. Bažant (2002) points out that if a small specimen size is selected the development of the fracture process zone is hindered by the boundary conditions. If on the other hand, a large specimen size is selected the crack does not form uniformly over the cross-section causing the sample to flex sideways, in which case the load condition at fracture is no longer purely uniaxial. This poses a problem for concrete mixes containing large fibres, such as steel fibres. For these mixes relatively large tensile specimens are required to ensure a fibre dispersion in the ligament area representative of the dispersion found in full-size structures. Direct tension tests on 300 mm long, 100 mm diameter cylinders were attempted as part of this study, but had to be abandoned. The specimens without exception cracked at the interface between the fixture and the cylinder. This indicated that the specimens did not fail in direct tension, but due to a stress concentration at the boundary. The results were therefore invalid and are not reported.

The splitting tensile test, also known as the Brazilian test, is typically performed on 150 mm diameter by 300 mm length cylindrical specimens. These dimensions are appropriate to create representative samples for most fibre reinforced concrete mixtures. Like the direct tension test though, the splitting tensile test is known to have a number of limitations. For normal strength concrete the empirically obtained split tensile strength can be expected to be 10 to 40 per cent higher than the actual uniaxial strength of the material (Olesen et al., 2006). Importantly for this study, Olesen et al. (2006) have shown that in the standard configuration the test cannot be used to obtain the tensile strength of FRC due to the ductility of the material.

The challenges in using the split cylinder test for both plain and fibre reinforced concrete are caused by the difference between the simple boundary conditions and linear elastic material behaviour assumed in the continuum mechanics model of the test, and the actual boundary conditions of the test and the non-linear material response. As part of this study an adjusted tensile splitting test procedure was developed to obtain a close estimate of the true tensile strength of fibre reinforced concrete. The methodology addresses the shortcomings of the

tensile splitting test for this purpose, by combining concepts introduced by various researchers in this field. The method can be summarized as follows: The linear elastic tensile stress calculation for the test is corrected for the influence of the width of the load strip by using the equation Tang (1994) recommended. The fracture mechanics size-effect, which is due to the quasi-brittle material behaviour of concrete, is reduced to acceptable proportions based on the recommendations by Rocco et al. (1999a, 1999b). Finally, the limit between linear elastic pre-crack behaviour and the ductile post crack behaviour of FRC is identified by monitoring transversal deformation perpendicular to the load direction during the test.

The calculation of the maximum principal stress in the splitting test is based on the two dimensional problem shown in Figure 3-7a.

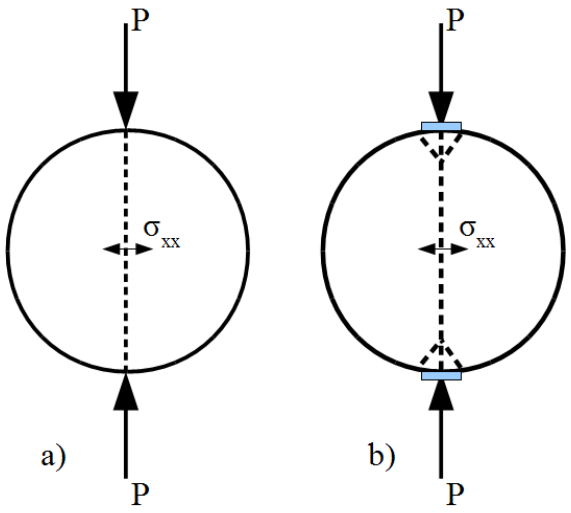

Figure 3-7a: Assumed load condition tensile splitting test, b: Actual load condition

The plane stress continuum mechanics solution for this problem provided by Timoshenko and Goodier (1970) allows calculation of the horizontal normal stress (σ_{xx}) along the loading axis of two equal and opposed point loads using Equation 3.1.

$$\sigma_{xx} = \frac{2P}{\pi D} \tag{3.1}$$

Where D is the specimen diameter and P is the magnitude of the point loads. A point load in the plane stress problem corresponds to a load per unit length of the specimen in the three

dimensional situation, which is how P is used throughout this section on tensile splitting tests. The load causes a uniform tensile stress state along the loading axis of the specimen. The actual loading condition in the splitting test setup (shown in Figure 3-7b) differs from the assumed situation of Figure 3-7a.

In reality the loads are introduced to the specimen by means of a loading strip with a certain width and not as point loads. The loading strip results in a non-uniform distribution of the normal stress along the loading axis of the specimen, with a compressive zone in the material near the contact area of the load strip. The size of the compressive zone depends on the size of the load strip and the condition leads to an overestimation of f_t obtained from Equation 3.1 (Rocco et al., 1999b). Tang (1994) corrected the linear elastic plane stress solution for the presence of a load strip with a finite width. Based on the correction by Tang (1994) the horizontal normal stress at the centre of the cylinder may be calculated using:

$$\sigma_{xx} = \frac{2P}{\pi D}\left[1-\left(\frac{b_1}{D}\right)^2\right]^{\frac{2}{3}} \tag{3.2}$$

Where b_1 is the width of the load strip. This correction results in a downward adjustment of the maximum stress of 4 % if the size of the load strip is within the specifications of ASTM 496 (ASTM, 2008b). The correction of the linear elastic load condition therefore accounts only for a small portion of the overestimation of f_t reported for splitting tensile tests.

A larger proportion of the difference between the splitting tensile strength and the true tensile strength is due to the quasi-brittle material behaviour of concrete and the related fracture mechanics size effect. Rocco et al. (1999a, 1999b) investigated the influence of the fracture mechanics size effect on the results of the tensile splitting test. Their analysis indicates that differences of up to 40 per cent in tensile strength can be found depending on the width of the load strip and the applied loading speed. In a later publication, Rocco et al. (2001) reported a 30 per cent difference in tensile strength values between much used international standards, i.e. ASTM C-469, ISO 4105 and BS 1881-117. They proposed that the split cylinder test can yield a true indication of the tensile strength as long as the width of the loading strip does not exceed 8 per cent of the diameter of the specimen and the speed of loading does not exceed 1.0 MPa/min (Rocco et al., 1999a).

The assumed fracture mode in the calculation of the tensile stress in current standard methods, using Equation 3.1, is rupture starting at the centre of the specimen. The crack would grow in the direction of the highest stress, i.e. towards the loading strips. In a study on mechanisms of rupture in the splitting test, Rocco et al. (1999c) found that this primary mode of failure, schematically shown in Figure 3-8a, is followed by secondary cracking, as shown in Figure 3-8b. This implies that after the tensile strength of the material is reached and a crack has formed in the centre of the specimen along the loading axis, the stresses redistribute and new highly stressed areas appear. By measuring the transversal deformation during the test, Rocco et al. (1999c) found that both the principal crack formation and secondary crack formation have a peak as shown in Figure 3-8c. The relative position of the peaks varies depending on material type and specimen geometry. In a situation where the secondary peak load exceeds the principal peak load, the tensile strength calculated using Equation 3.1 would be invalid.

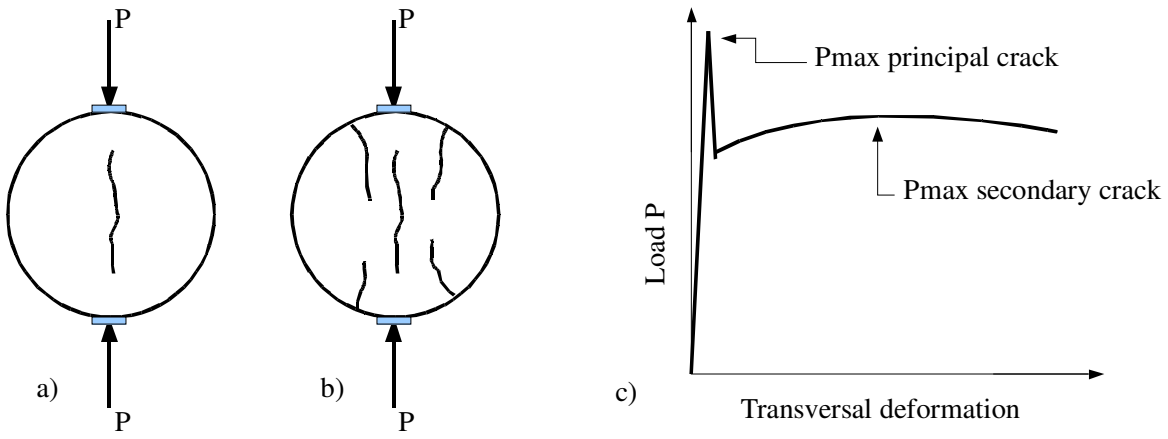

Figure 3-8: a: Principal crack formation, b: Secondary crack formation, c: schematic load-deformation curve (after Rocco et al., 1999c).

Adjusted split cylinder tests were performed to obtain the tensile strength for the high performance fibre reinforced concrete mixes under study. The test configurations used for the study are shown in Figure 3-9. For the experiments on mixes A, B and D the spring loaded LVDTs were held by fixtures mounted to the base plate in the test machine as shown in Figure 3-9a.

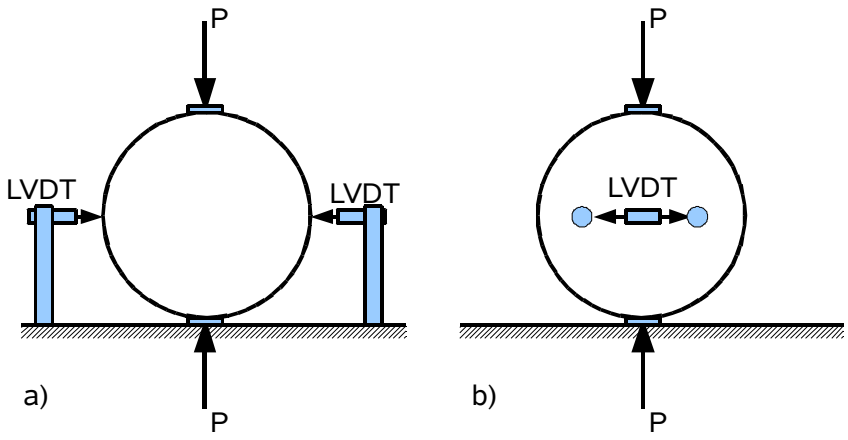

Figure 3-9: a: Initial test configuration, b: Improved test setup

The LVDTs were positioned at centre line of the specimen and at the centre of its length. A more advanced measuring system was developed for the tests performed on mix E. For this last mix the transversal deformation was measured using LVDTs mounted to datum points which were glued to the specimens. Measurements were taken on both sides of the cylinder.

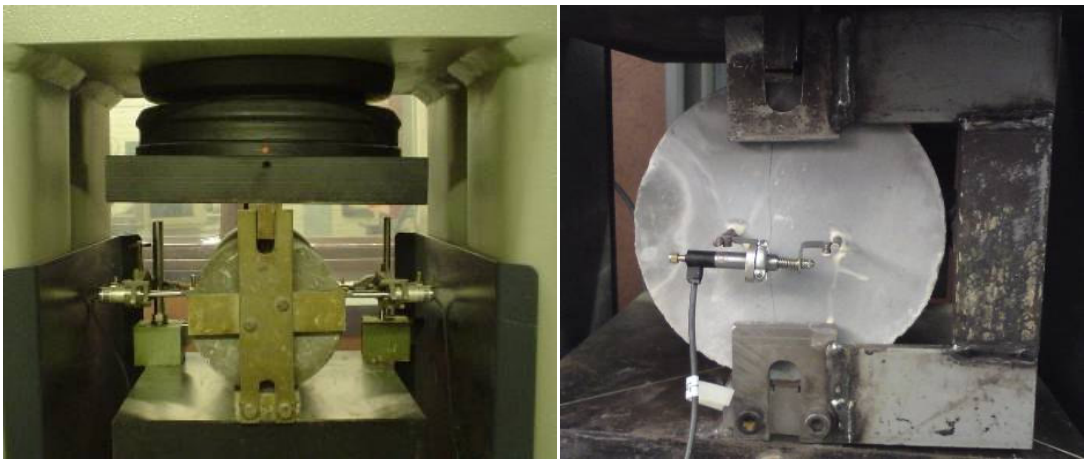

Figure 3-10: Photos of split cylinder test setup

The setup is shown schematically in Figure 3-9b. Photos of both test configurations are shown in Figure 3-10. In accordance with the recommendations for reduction of size effect

by Rocco et al. (1999a), a loading strip of 12mm width (8 % of the diameter) was used and the loading rate was kept at 1 MPa per minute for all tests.

The measurement of transversal deformation using LVDTs has a limited precision, especially when the fixtures are mounted to the base plate as was done for the first mixes. The objective however is to identify the point at which the linear elastic stress distribution ceases to exist, for which purpose the method was found to be adequate.

For the plain concrete (Mix D), measurement of the transversal displacement was deemed unnecessary to obtain reliable results. Therefore, the standard test configuration in accordance with ASTM C-469 was used.

3.3 Selection of numerical simulation methods

An overview of relevant fracture mechanics approaches was provided in Section 2.5 of this document. Importantly, Elsaigh (2007) had previously used a smeared crack approach to model fracture in similar materials as part of his PhD studies at the University of Pretoria. Elsaigh reported considerable difficulty in implementing the highly non-linear fracture behaviour of the material in the MSC.Marc (Mentat, 2003) finite element software.

The selection of the numerical methods for this study was largely dictated by the availability of suitable methods. The study employs both discrete and smeared crack approaches to simulate fracture. Two software platforms were used at different stages of the study. Initially, the open source FEM framework OpenSees (OpenSees, 2008) was used for the modelling of fracture in beams. In OpenSees software discrete fracture was modelled in two dimensional space by means of the Embedded Discontinuity Method (EDM). When, at a later stage in the study, modelling of fracture in three dimensional space became required, the commercial FEM code Abaqus (Abaqus, 2009) was acquired. In Abaqus, a cohesive fracture approach was used for the simulation of cracking in the three dimensional flexural disk tests as well as two dimensional simulation of the tensile split cylinder test. Earlier attempts to simulate the splitting test using the EDM approach had been unsuccessful. Due to the large “snap back” in the response of the cylinder when a crack is formed the calculation using OpenSees software failed to converge. Abaqus can be set to automatically adjust the number of iterations per load step and this made simulation of the split cylinder test possible. A simplified model of a

pavement structure is also analysed in Abaqus, using a cohesive crack damage model for the concrete slab.

3.3.1 Modelling of flexural beam tests with EDM in OpenSees

As part of a work visit to the University of California at Davis, the author assisted in the validation of the EDM code implemented in Opensees as later published by Wu et al. (2009). The EDM is based on work by Simo et al. (1993), Oliver (1996a, 1996b) and Sancho et al. (2007).

The EDM takes its name from embedding the Strong Discontinuity Approach (SDA) within finite elements. A strong discontinuity is typified by *"the occurrence jumps in the displacement field appearing at a certain time, in general unknown before the analysis, of the loading history and developing across paths of the solid which are material (fixed) surfaces"* (Oliver, 1996b). Essentially, EDM adds internal nodes to cracked elements. The extra degrees of freedom associated with these internal nodes are used to describe the displacement jumps (both in shear and opening) across crack faces. Internal nodes do not show up in the global stiffness matrix for finite element analysis, allowing the flexibility of adding them or removing them in any element without affecting the overall analysis. An advantage of SDA and therefore EDM over more conventional discrete crack models, such as cohesive crack interface element models, is that it allows cracks to propagate through elements, in other words, independent of nodal positions and element boundaries. EDM differs from so-called smeared crack or crack band approaches in that it forms a discontinuous cracked surface. The use of displacement rather than strain to enforce softening has as important advantage that EDM does not suffer from mesh size dependencies. The constitutive equations of the EDM formulation used for the present study are as published in Wu et al. (2009). The methodology uses the efficient crack adaptation technique to prevent crack locking developed by Sancho et al. (2007).

The cracking function in the EDM is based on the principles of the cohesive crack model introduced by Hillerborg et al. (1976), discussed in Section 2.5. According to the cohesive crack approach a crack is induced when the stress in the material reaches the tensile strength (f_t) of the material. After the crack has formed, stresses will still be transferred over the crack, however, the amount of stress transferred reduces as the crack width increases.

In the flexural beam tests, crack growth due to shear stress should be negligible. The characterization of shear damage evolution requires specialized testing, not undertaken as part of this study. The EDM code used in this study does however allow for tension, shear and mixed mode fracture to occur where applicable. In the implementation, the shear softening curve is exactly the same as tension softening curves. The traction across the crack faces is the vector sum of the crack opening (tension) and crack sliding (shear) traction. The total traction vector has the same direction as the relative opening movement. The magnitude of the traction vector is determined by the softening function using the magnitude of the total crack opening displacement.

The EDM was implemented in OpenSees using three-node triangular elements. The model geometry and meshes were created using Gmsh (Geuzaine and Remacle, 2009) pre- and post-processor software. Routines in this opensource software were adjusted by the author to allow the creation of mesh definitions that are compatible with the OpenSees code.

A typical example of a two dimensional mesh used in the simulation of a TPB test on a notched specimen is shown in Figure 3-11. In principle it is possible to use embedded discontinuity elements for the entire geometric model. This will allow the crack to form at the position in the specimen with the highest tensile stress. In simulation of the notched TPB tests however, the crack will always form directly above the notch. To make the calculation more efficient, the elements with embedded discontinuity were arranged in a vertical band above the notch as shown in Figure 3-11. A characteristic length of 1.0 mm was used for the EDM elements in the analysis of all specimens. The remainder of the material is modelled using LE bulk elements.

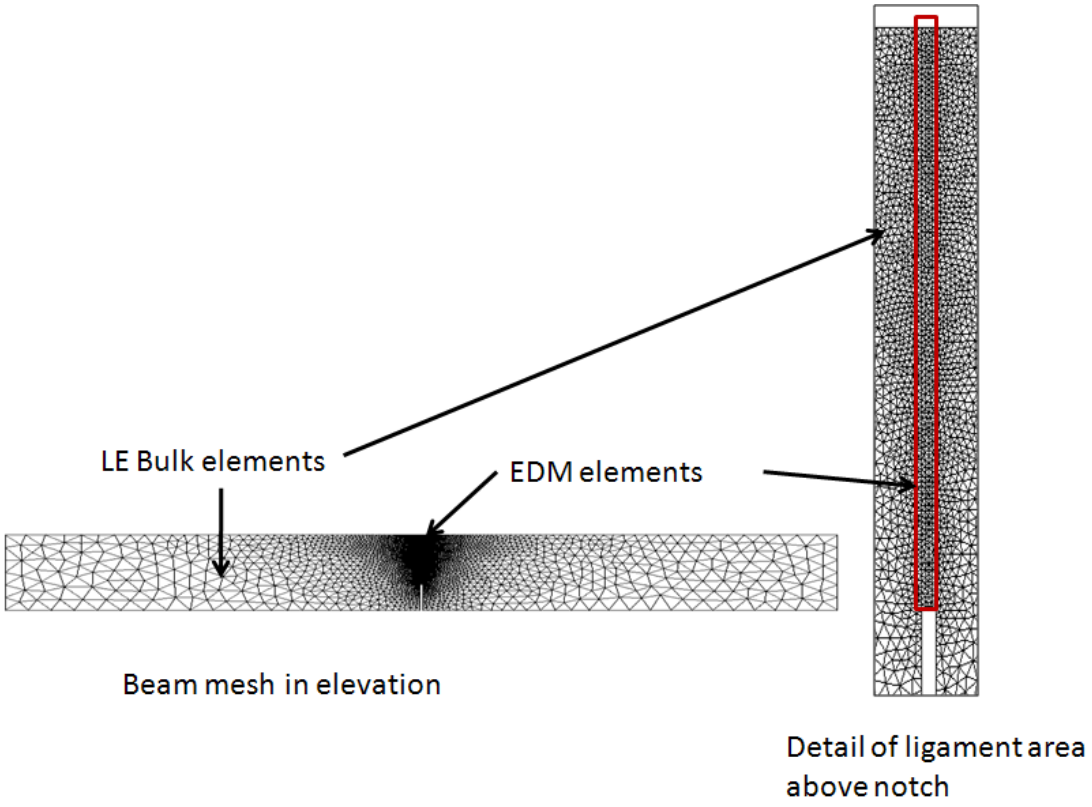

Figure 3-11: Example of TPB finite element mesh

3.3.2 Modelling of centrally loaded panels and split cylinder tests using Abaqus

The commercial FEM software package Abaqus includes a number of fracture mechanics models that can be applied to concrete. Amongst these is a brittle cracking model intended specifically for the simulation of fracture in concrete. The approach follows the smeared cracking assumption as discussed in Section 2.5.5. Damage evolution however, takes place using the cohesive crack model by Hillerborg et al. (1976) rather than strain softening. This to remedy the mesh size sensitivity problem of conventional smeared crack approaches (Dassault Systèmes, 2009). Because the Abaqus brittle crack model uses the cohesive crack principle for damage evolution in the principal tensile stress direction, the same softening functions can be used for the numerical simulation in both Abaqus and OpenSees.

In contrast to the EDM in which both shear and tension are handled using a crack width softening function, the brittle cracking model in Abaqus has a separate strain softening function for shear. The reason for the combination of a mode II strain softening model with a mode I displacement softening model, instead of displacement softening for both modes is not clear from the documentation. To ensure that the response of the Abaqus model in shear

was similar to that in the EDM simulation, the shear strain softening function was defined in accordance with the function in Equation 2.15. This equation relates the strain softening in smeared crack models to the softening as function of crack width in cohesive crack models.

Figure 3-12 shows the geometry of the numerical model for the tensile splitting test. Owing to symmetry, only a quarter of the cylinder test needs to be modelled.

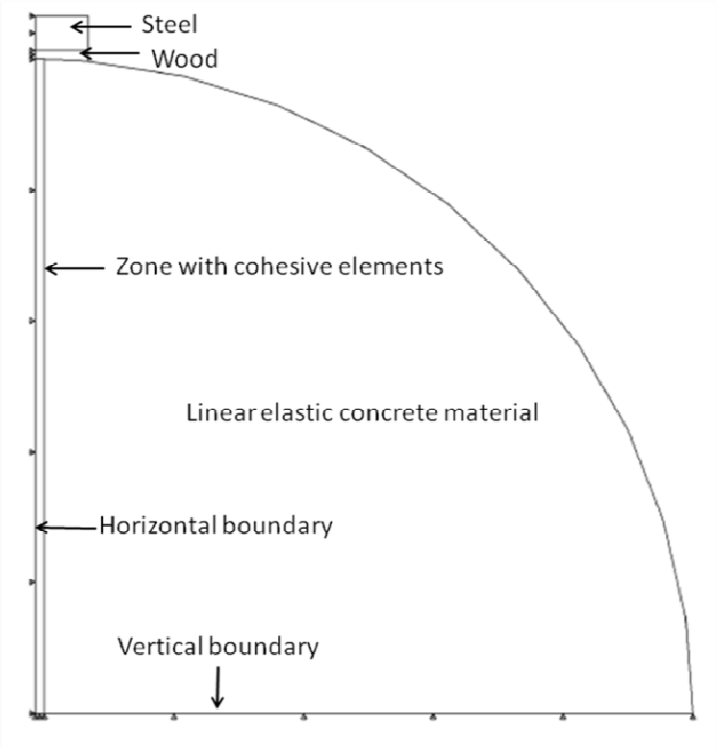

Figure 3-12: Geometry of numerical model for splitting test

A vertical zone of 1 mm x 1 mm sized, standard Abaqus plane stress cohesive elements with the brittle fracture model was provided along the loading axis. The brittle fracture elements behave linear elastically based on the values for E and υ obtained for the material until the tensile strength is reached, after which damage evolves as defined by a cohesive crack model to be developed for the material in Chapter 5. The behaviour of the remainder of the concrete section is simulated using plain stress linear elastic bulk elements. To accurately simulate the load introduction to the specimen, the steel loading strip and the plywood interface strip are also modelled. An E value of 210 GPa and υ value of 0.25 were assumed for the steel. Values of E= 5 GPa and υ= 0.3 were assumed for the plywood.

Numerical simulation of the centrally loaded disk test was also performed using Abaqus. The layout of the test is shown schematically in Figure 3-13a. Owing to symmetry, only one sixth of the disk needs to be modelled. The geometry and boundary conditions are shown in Figure 3-13b. This simplification considerably increases the efficiency of the numerical simulation. The disks are analysed both using LE material properties and a fracture mechanics damage model. For the LE analysis all elements used for the model were LE bulk elements. For the fracture mechanics analysis, the LE bulk elements in the areas indicated in Figure 3-13b were replaced by elements with a fracture mechanics damage definition. The support point is connected to a surface corresponding to the area of the transfer plate under the panel using a kinematic rigid coupling. Standard Abaqus 8 node brick elements of the C3D8R type were used for the mesh. The characteristic size of the elements throughout the model is 5 mm, with exception of the area around the support, away from the highly stressed areas, where a size of 15 mm was used.

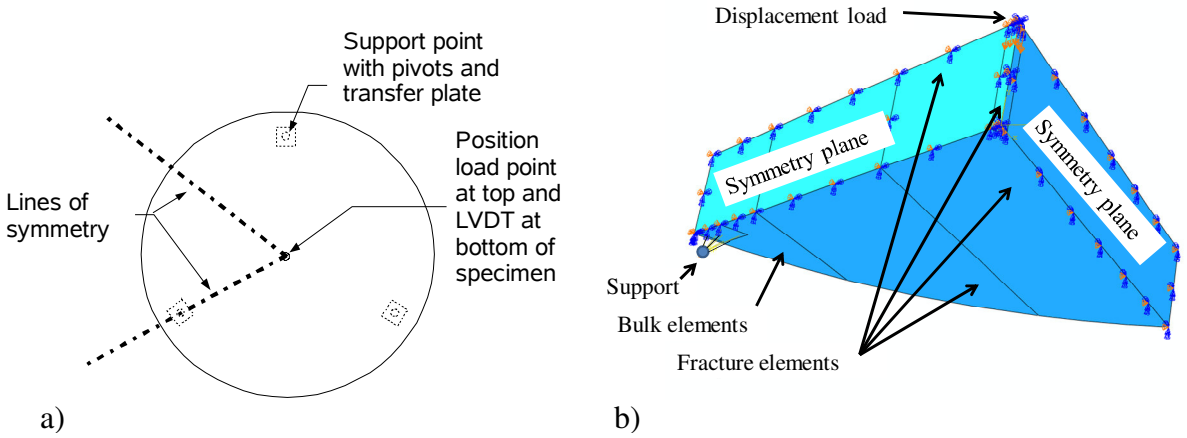

Figure 3-13a: Geometry of test, b: Geometry and boundary conditions of model

3.4 Discussion on the methodology

The research methodology was developed to test the different hypotheses of this work. The first proposition is that high performance fibre reinforced concrete material will exhibit a strong size effect due to its distinctly non-linear behaviour in fracture. The size effect for the high performance fibre reinforced concrete material under monotonic and cyclic loading is quantified using a FPB tests on beams of different sizes, but of a constant geometry. Tests on

centrally loaded disks of different sizes under monotonic loading are included in the experimental matrix for size effect as well,

According to the second proposition, fracture mechanics can be used to more accurately and precisely predict the peak load and flexural behaviour of elements of a different size and geometry. To test this hypothesis, fracture properties are determined from TPB tests on weight corrected beam specimens with a notch. The tensile strength is obtained from an adjusted tensile splitting test procedure. The fracture mechanics properties obtained from these tests are then used in the definition of a cohesive crack function for the material. The cohesive crack model, or softening function, is implemented in finite element software to simulate the fracture behaviour observed in the experiments for specimens of different sizes and geometries.

The third proposition states that the accuracy, and possibly the precision, of fatigue prediction models can be improved through the use of fracture mechanics concepts. To test this hypothesis, cyclic tests are performed on FPB beam and centrally loaded disk specimens. The behaviour of the material in the cyclic loading tests is compared to the behaviour in the monotonic loading experiments. The aim is to calibrate a conventional and a fracture mechanics based prediction model against the fatigue results of the FPB beam tests. These models will then be used to predict the fatigue life of the centrally loaded disks and of beams of different sizes.

The results for the tests of the three propositions will be used to evaluate the main hypothesis of the study that the accuracy of design models for the high performance fibre reinforced concrete used in UTCRCP can benefit from the inclusion of fracture mechanics concepts.